PHYSICAL MECHANISMS CONTROLLING UPPER TROPOSPHERIC WATER VAPOR AS REVEALED BY MLS DATA FROM UARS

IN-47

FIRST PROGRESS REPORT

Under NASA UARS Science Grant NAG 5-6710

For the period December 1, 1997 through November 30, 1998

Principal Investigator: Professor Reginald E. Newell
Massachusetts Institute of Technology
77 Massachusetts Avenue, 54-1824
Cambridge, MA 02139

Submitted to: Dr. Anne Douglas, Technical Officer
Code 916
National Aeronautics & Space Administration
Goddard Space Flight Center
Greenbelt, MD 20771

By: Professor Reginald E. Newell
Dept. of Earth, Atmospheric and Planetary Sciences
Massachusetts Institute of Technology
77 Massachusetts Avenue, 54-1824
Cambridge, MA 02139
Phone: (617) 253-2940
FAX: (617) 258-9819
E-Mail: newell@NEWELL1.mit.edu

Abstract

The seasonal changes of the upper tropospheric humidity are studied with the water vapor data from the Microwave Limb Sounder on the NASA Upper Atmosphere Research Satellite, and the winds and vertical velocity data obtained from the European Centre for Medium-Range Weather Forecasts. Using the same algorithm for vertical transport as that used for horizontal transport (Zhu and Newell, 1998), we find that the moisture in the tropical upper troposphere may be increased mainly by intensified local convection in a small portion, less than 10%, of the whole area between 40°S to 40°N. The contribution of large scale background circulations and divergence of horizontal transport is relatively small in these regions. These dynamic processes cannot be revealed by the traditional analyses of moisture fluxes. The negative feedback suggested by Lindzen (1990) also exists, if enhanced convection is concentrated in the tropics, but is apparently not the dominant process in the moisture budget.

1 Introduction

The effect of increasing sea surface temperature (SST) on the change of moisture in the upper troposphere has received wide interest, since the hypothesis of a possible negative feedback was proposed by Lindzen (1990). This hypothesis was detailed by Sun and Lindzen (1993). They argued that the cumulus-induced time and zonal mean large scale subsidence could be increased if sea surface temperatures increased, while the contribution of eddy fluxes would be negligible. According to Ras-

Work under this proposal has been reported during the past year at two scientific meetings: the UARS Science Team Meeting held March 16-18, 1998 in Pasadena, California and the International SPARC Water Vapor Workshop held August 26-28, 1998 at Boulder, Colorado. Dr. John Cho and Mr. Yhong Zhu represented our group at the first meeting and Mr. Zhu attended the SPARC Workshop.

We have drawn what we think are significant conclusions from our analyses during the first year and a paper was prepared and has been discussed with Dr. Joe Waters and/or Dr. William Read of JPL at the Science Team meeting in March, at MIT when Dr. Read attended the AGU meeting in Boston in May 1998, at JPL when Professor Newell attended a PEM-Tropics Science Team meeting at Edwards Air Force Base, CA and in late June 1998, and when Mr. Zhu attended the SPARC workshop. This paper was submitted to the Journal of Climate in August 1998. A copy of this paper is attached as Appendix 1.

Points worthy of note are that tropical convection produced a larger flux of water vapor into the upper tropical troposphere in the December 1991-February 1992 period, an El Niño, than in the following year and that in the tropical region, treated as two 20° latitude subdivisions (20°-Equator), the convective contribution always outweighed the convergence of the horizontal transport. Even in latitude belts 20° on either side of these regions there was generally a net positive contribution to the UTH. Vertical fluxes were obtained using ECMWF winds and a new algorithm based on our work on atmospheric rivers.

We are now working on the different mechanisms that may operate in the tropopause region. Does the middle latitude forcing in the upper tropical troposphere contribute differently than the regions below (215, 316 and 464 hPa)? For this we need in addition to the 147 hPa data,

MLS data at 100-10 hPa. We understand these are now being processed by the group at the University of Edinburgh.

The MOZAIC data have recently been made available with water vapor data corrected and we expect to compare these with UARS MLS H_2O data at and below 215 hPa. This work will take place in the first quarter of 1999.

As we stated in our revised work plan we have examined some of the MOZAIC data for heating rates and radiative fluxes. We find that the results are strongly dependent on the fine details of the profiles and are planning to expand this work. There are significant changes in the rates and fluxes when the overhang of UTH from the tropical convection moves away from the convective source and we will be investigating these changes in detail.

Appendix 1

Factors controlling upper troposphere water vapor

Yong Zhu, Reginald E. Newell

Department of Earth, Atmospheric and Planetary Sciences, MIT, MA

02139

William G. Read

Jet Propulsion Laboratory, California Institute of Technology, Pasadena,

California

August 17, 1998

Submitted to J Climate

musson (1972) and Peixoto and Oort (1992), the water vapor transport by time and zonal mean flows is dominant only below 500 hPa; the fluxes carried by stationary eddies and transient perturbations may be greater in the upper troposphere. A general circulation model used by Allam and Tuck (1984) showed that the meridional mass fluxes in the upper troposphere were dominated by the time and zonal mean flows at all latitudes, while the moisture flux carried out by transient and stationary eddies were comparable with the flux contributed by the time and zonal mean flows, except in the tropical regions. Del Genio *et al.*, (1994) reported that the upper tropospheric moisture feedback in their general circulation model is positive, since the drying by the mean Hadley cell subsidence was offset by the moistening resulting from convergence of the vertical eddy flux.

The Microwave Limb Sounder (MLS) on the NASA Upper Atmosphere Research Satellite (UARS) provided unique satellite datasets of upper troposphere humidity (UTH), which includes measurements in the presence of cirrus (Read *et al.*, 1995). A new version of the humidity data (V490) is now available at 4 pressure levels: 464, 316, 215 and 147 hPa, based on the relative humidity with respect to ice. The data coverage is continuous from 34°S to 34°N, with a change every 36 days between 34°N-80°N and 34°S-80°S. The discussion of the new data and comparisons with other datasets has been given by Sandor *et al.* (1998). We will use the MLS humidity data together with the European Centre for Medium-Range Weather Forecasts (ECMWF) winds and vertical velocity to study the seasonal variations of UTH and the related dynamic mechanisms.

2 Positive or negative feedback?

Some general circulation models have yielded a positive feedback of UTH from increasing SST (Cess *et al.*, 1990; Del Genio *et al.*, 1994). On the other hand, Chou (1994) and Fu *et al.* (1997) argued that enhanced tropical convection reduced the UTH in the adjacent subtropical areas, shown by data analyses and model results. These consequences appear to be in conflict with each other, but both may be right.

Figure 1 compares the differences of SST and MLS UTH between an El Niño season in 1992 and a pre-La Niña season in 1994. In the tropical Pacific, the ocean surface was generally colder over the western part, but warmer over the eastern part in early 1992. Two areas of negative SST difference occurred also on both sides of the warm pool. A similar pattern is found also in the difference of MLS UTH. This feature suggests a positive correlation between the UTH and local SST, as reported with different datasets by others (Raval and Ramanathan, 1989; Rind *et al.*, 1990; Soden and Fu, 1995). Now, if we compare the low MLS UTH over the eastern subtropical Pacific with the warm tropical ocean water beneath, a negative correlation results. Certainly, the negative correlation does not mean that the local correlation between UTH and SST was also negative. Higher UTH in one region is often connected with deep convection in a region far removed as seen in an example we provided elsewhere (Newell *et al.*, 1997, Figure 5). This gives a limitation on the study of the greenhouse effect in terms of the feedback of UTH in the tropical El Niño events. While the high relative humidities ($> 80\%$) in Figure 1 spanning the latitudes from about 20°N to 20°S are based on ECMWF analysis, they were verified by the presence of cirrus observed by airborne lidar from the intertropical

convergence zone at about 10°S to north of Guam at 14°N (Newell *et al.*, 1996). One particular general circulation model, which produced the negative feedback of subtropical UTH to the intensified deep convection during the 1987 El Niño (Fu *et al.*, 1997), could also produce positive feedback to an increase of SST (Cess *et al.*, 1990). We will discuss in Section 5 the dynamical processes responsible for the positive and negative feedbacks.

3 UTH fluxes by ECMWF winds

The time and zonal mean meridional fluxes of water vapor may be partitioned into (Rasmusson, 1972)

$$[\overline{vq}] = [\bar{v}][\bar{q}] + [\bar{v}^*\bar{q}^*] + [\overline{v'q'}] \,, \tag{1}$$

where, v is the meridional wind component, and $q = \rho_w/\rho_a$ is the specific humidity (ρ_a and ρ_w represent the densities of air and water vapor, respectively). Analogously, the vertical fluxes may be written as

$$-\frac{1}{g}[\overline{wq}] = -\frac{1}{g}([\bar{w}][\bar{q}] + [\bar{w}^*\bar{q}^*] + [\overline{w'q'}]) \tag{2}$$

in the pressure coordinates, where $w = dp/(dt)$ and g is the gravitational acceleration. The three terms on the right-hand sides of the two equations are so called, respectively, the fluxes by the zonal mean flow, stationary eddies and transient perturbations. The temporal mean is denoted by an overbar; the zonal mean is put in the square brackets, and the prime and asterisk indicate the deviations from the temporal and zonal means, respectively. Figure 2 gives the zonal distributions of the seasonal mean meridional and vertical MLS water vapor fluxes carried by ECMWF winds and vertical velocity in 1992 and 1993. The

meridional fluxes are integrated from 464 hPa to 147 hPa, for example

$$Q_\phi = \frac{2\pi a}{g} \int_{147hPa}^{464hPa} [\overline{vq}] \cos\phi \ dp \ , \tag{3}$$

where a is the Earth's radius and ϕ is latitude. The vertical fluxes are evaluated on 464 hPa. To use the same units as that of the meridional flux, (2) may be integrated to give

$$Q_w = -\frac{2\pi a^2}{g} \int_{\phi_1}^{\phi_2} [\overline{wq}] \cos\phi \ d\phi \ . \tag{4}$$

The meridional flux by the zonal mean flow was strongest in the tropical region, which transports moisture across the equator from the summer hemisphere to the winter hemisphere. In the northern summer, the southward flux was stronger than the northward flux at the equator. In the subtropical regions from latitude 20° to 40°, the mean flow transports moisture poleward, except in the summer northern hemisphere. The total transport was poleward, showing divergence from about 10° latitude, and dominated by transient perturbations in the subtropical regions. The stationary eddy flux was comparable with the mean flow flux in magnitude except near the equator. It was generally northward in northern winter, but southward in northern summer. This implies that the seasonal phase changes in the stationary wind perturbations may not be correlated to the seasonal changes of humidity field.

The patterns for 1993 (Figure 2b) are quite similar to those for 1992 (Figure 2a), with both showing smallest poleward fluxes in the Northern Hemisphere summer. In that season the water vapor flux divergence from 10°N is composed of a small transient eddy flux northwards and a mean flow component southward into the Southern Hemisphere. For the four 1991-1992 seasons 342 days were sampled, for 1992-1993 332 days were sampled, while for 1993-1994 272 days with three months

being 16 or less and 6 months less than 19 days. To avoid this sampling problem, we confined the analyses to the first two years.

The mass fluxes may be evaluated by inserting $q = 1$ (ie. $\rho_a = \rho_w$) in (2) and (3). The time and zonal mean of mass transport is completed only by the mean flows, as the transient and stationary eddies have no net contribution. So, there is an essential difference between the vertical transport of mass and moisture represented in the pressure coordinates, as the latter is a nonlinear process but the former is linear. The mean total vertical mass flux may be given simply by the zonal and time mean flow flux, and the direction of moisture transport by the mean Hadley cell (shown by the blue curves in Figure 2c, 2d) is also the direction of total mass transport.

The ascending branch of the mean Hadley cell produced the largest upward water vapor flux in the middle troposphere (Figure 2c, 2d), while the mean descending branch carried the moisture downward. The transient perturbations and stationary eddies pushed water vapor upward (ie. downgradient in the humidity field) at almost all latitudes. The amount of eddy transport in the subtropical regions was comparable with that of the mean Hadley cell transport, so that the total moisture transport could be opposite to the mean flow moisture transport or to the mass transport (eg. Southern Hemisphere winter at 10°S), or, in some cases, close to zero (eg. Northern Hemisphere winter 15°N-25°N). Both 1992 and 1993 give the same patterns with the tropical upward fluxes being higher in December 1991-February 1992, associated with El Niño in the tropical region.

4 Seasonal changes in UTH

The seasonal changes of UTH may give an example of the feedback to the surface heating. Figure 3 shows the MLS water vapor column content in the layer from 316 hPa to 147 hPa. The values may be underestimated in the tropics, as the mixing ratios may be lower than the balloon sonde data on 464 and 316 hPa when the vertical column is very moist (Sandor *et al.*, 1998). However, the displayed layer seems remarkably wetter than the layer of 300-100 hPa measured from SAGE II and analysed by Chiou *et al.*, (1997). The maximum content was found over the summer tropical areas around 10° latitude. The moisture over the subtropical regions increased nearly 100% from winter to summer in both hemispheres. This was unlikely produced by the interhemispheric transport, as the fluxes at the equator were towards to the winter hemisphere (Figure 2a, 2b).

The first half year of 1992 was accompanied by El Niño over the central Pacific. The zonal mean water vapor content was slightly higher near the equator, compared with the normal year of 1994. Although there were relatively dry patches on the both sides of the warm pool in the El Niño season (Figure 1), the moisture in the whole belts was not significantly lower than in the normal year. From June to August, 1994, the upper troposphere in La Niña season was generally drier than in 1992. It should be noted that July in 1994 had only 16 days of data, and June 1992 only 18 days. The dryness in the two transition seasons was also obvious in the MLS satellite data.

The annual means were slightly higher in the Northern Hemisphere than in the Southern Hemisphere for the two years. The annual mean temperatures in the lower troposphere and on the sea surface are also

higher in the northern tropical and subtropical latitudes than in the corresponding southern latitudes (Peixoto and Oort, 1992). So, the positive correlation between UTH and SST is also a long term mean feature.

5 Dynamic processes of UTH variations

From Riehl and Malkus (1958), nearly all upward heat and mass transport in the tropics takes place in tall cumulonimbus clouds. These convective clouds are a kind of transient perturbation, which have a lifetime shorter than that of the baroclinic cyclones at the middle latitudes. However, the vertical transient flux shown by Figures 2c and 2d was negligibly small compared with the mean flow flux in the tropics. So, the statistics in Figure 2 may not represent the real physical processes in the atmosphere, and may not reveal the relation between deep convection and large scale subsidence.

It was argued (Zhu and Newell, 1998) that the total meridional water vapor flux in the whole atmosphere may be accomplished by 4 or 5 atmospheric rivers. Thus, the transient flux calculated with the traditional algorithm may be underestimated. Palmén and Newton (1969) pointed out that the slow mean tropical circulation should be interpreted as the statistical result of the vigorous vertical motions in convective clouds that penetrate to the upper troposphere only in a very small portion of the total region. Thus, the so called zonal mean flow fluxes in (1) and (2) are contributed more or less by transient and local processes. This can be seen from Figure 4, which gives the vertical fluxes of water vapor across 500 hPa over a tropospheric river, evaluated

with ECMWF data at 12Z on January 4, 1992. A rapid developing cyclone, termed a bomb, related to this river has been discussed by Zhu and Newell (1994). Only 4 or 5 of the rivers along a typical middle latitude in the daily maps may complete the total vertical transport of water vapor at that latitude.

We will pick up 10 percent of the grid points at each latitude from 40°S to 40°N, which had the strongest vertical velocities on 464 hPa in the daily ECMWF datasets, and define this as the convection. This number is based on the previous work (Zhu and Newell, 1998). The rest is called the background flow. The vertical fluxes by the convection and background flow is displayed in Figure 5. Although the large scale ECMWF data may underestimate the convective velocities, the plotted convective flux is stronger than the background flux. It is positive at all latitudes, and accounts for the major part of total flux. The convective upward transport was peaked at the summer tropical regions, where the strongest divergence of horizontal flux took place as shown by Figure 2a. The downward transport was contributed by the background flows only.

The vertical influxes from the new algorithm are summarized in Table 1, which are evaluated from (4) on 464 hPa for Table 1a and 1b and on 316 hPa for Table 1c, assuming that the vertical fluxes across the tropopause are negligibly small. The convective flux in the tropical regions (20°S-20°N) was extremely strong in the first half of 1992 (Table 1a), which was in an El Niño period; the induced large scale subsidence reached the peak values in the subtropical regions. The couplings between strong convection and large scale subsidence are indicated by the boldface numbers in the table. These facts support the

hypothesis of negative feedback. In the normal year without El Niño (Table 1b), strongest convection in the large area from the equator to 40° of latitude took place in the summer hemisphere, and was weaker than the southern summer convection during the 1992 El Niño period. So, the induced subsidence was also weaker. Table 1b shows also that the convective flux in the northern subtropical region together with the induced downward fluxes on the two sides in the fall was the strongest during 1993 and was stronger than in 1992. This result is uncertain, as only 11 days were sampled in October 1993.

The upper troposphere was not dried by the enhanced subsidence in summer as it was overwhelmed by the convective flux. Tables 2a and 2b give the meridional and vertical influxes of MLS water vapor into the layer from 464 hPa to 150 hPa in 1992 and 1993 respectively. In general, the convergence of the meridional fluxes were much less than net vertical influxes in the upper troposphere. So, the interhemispheric transport may not be critically important for the local balance of UTH. The maximum vertical flux and net influx occurred in the summer over the large area from the equator to 40° of latitude. El Niño could also have an effect on the net influx, as the influx was stronger in the first half of 1992 than in the first half of 1993. The annual mean influx in 1992 was also stronger. Comparing with Figure 3, we find that the high water vapor content in the summer hemisphere was related to the maximum influxes contributed mostly by local convection. That the annual mean UTH in the Northern Hemisphere was higher than in the Southern Hemisphere was also correlated to the bigger influxes.

A similar analysis has been carried out for the layer from 316 hPa to 147 hPa. The results for 1992 appear in Table 1c. The pattern is

the same with absolute magnitudes of the fluxes smaller as would be expected, because both vertical air motion and humidity diminish with altitude. Furthermore, the MLS water vapor value is underestimated relative to radiosonde data by a larger factor at the higher values at 316 hPa than at 464 hPa, though the differences may not yet be well enough established to claim that this is the only reason for the contributed differences observed here (Read *et al.*, 1999). The large scale subsidence flux does not decrease as much at 316 hPa as the convection. Divergence of the vertical fluxes in Table 1c are compared with horizontal flux divergence in Table 2c for the 316-147 hPa layer and the 1992 year. The general pattern is the same with the vertical flux still dominating over the horizontal flux for the higher layer. The patterns revealed are quite stable from one year to the next and for the two upper tropospheric layers.

6 Slantwise convection

As discussed by Eady (1950) and Palmén and Newton (1969), the large scale circulations at the middle latitudes may be termed slantwise convection, in which the vertical motions are a few centimeters per second compared with the horizontal wind speeds of tens of meters per second. This is also the situation for the large scale circulation in the subtropical regions, except that the trajectory slopes in this case are larger in the meridional direction than in the zonal direction. The monthly mean winds in ECMWF data for January 1992 show a westerly subtropical jet over the North Pacific at around 32°N, with maximum speeds of 41 m/s at 500 hPa and 78 m/s at 200 hPa. These values were not the same

as shown by Figure 6a discussed later on, as they did not occur at the plotted longitude. The jet in the Southern Hemisphere around 24°S was weaker. The meridional velocity of the mean circulation is also much greater than the vertical velocity. As commented by Green *et al.* (1966), the circulations of large scale mid-latitude convection may extend near the surface into much lower latitudes than is generally appreciated. Some of the local convection defined in the preceding section could be the slantwise convection in the daily fields, if the trajectory slopes were relatively small. The vertical cross-sections along the trajectories of the monthly mean winds plotted from ECMWF data show that the differences between the slopes of the trajectories and isentropic surfaces are very small in the subtropical regions.

Thus, the moisture transport in the atmosphere depends not only on the vertical motions, but also on the horizontal fluxes. Figure 7 gives two examples of the local correlations between vertical motions and humidity changes, plotted from ECMWF data. The large scale subsidence around 20N, 65E and 22.5S, 70E, respectively, induced by tropical deep convection and the Asia Monsoon did not dry the upper troposphere. The increases of humidity in these two examples were contributed by horizontal transport. When the humidity surface is steeper than the isentropic surface, the large scale downward motion on the isentropic surface may moisten the local atmosphere.

The subtropical atmosphere may be dried efficiently by the equatorward flows which come from the low stratosphere through a folded tropopause just above and below the subtropical jets. A picture of the slantwise convection in the subtropical regions is given by Figure 6. The maximum speeds of the descending and ascending flows in the time

mean cross-section was -1.9 cm/s and 2.5 cm/s, respectively. The daily values could be 5 times bigger over the Pacific Ocean. The adiabatic heating in the subsidence is much larger than radiation cooling. So, the straightforward downward motion may not be the best representation for the large scale circulation pattern in the subtropics, except in the thermally unstable tropical atmosphere.

It is noted that the vertical and horizontal components cannot be measured directly from the Figure 6, as the vertical and horizontal scales of the cross-section are different. The angles between the velocity vectors and the isentropic surfaces in the cross-section may represent approximately the angles in the three dimensional space, if the isentropic surfaces do not tilt strongly in the direction normal to the cross-section. The vectors had large angles to the isentropic surfaces in the stratosphere, because the zonal tilt of the isentropic surfaces was relatively large and the flows were nearly normal to the cross section. If plotted along with the trajectories in the domains out of the tropics, the angles become negligibly small as shown by Finger 6c.

The stratospheric intrusion in the Northern Hemisphere produced a deep tongue in the MLS humidity field, together with a potential vorticity tongue below. The stratospheric air may reach the tropical areas in the lower troposphere. If there is a positive correlation between increases of tropical deep convection and mid-latitude baroclinic activities, the intensified stratospheric intrusion may produce a negative anomaly in the subtropical humidity field. The drying process was also evident below the southern jet. As a result, the equatorward horizontal gradients in the humidity field increased sharply in the subtropical upper troposphere.

However, this finding does not mean that the feedback from the increase of SST over the globe is also negative. As the time mean large scale circulations are characterized by slantwise convection, and the horizontal gradient in the humidity field is large, the effect on water vapor transport cannot be studied with an one dimensional model.

7 Conclusions and discussion

The zonal mean MLS water vapor column content in the upper troposphere increased with increasing sea surface temperature in an annual cycle in the tropical and subtropical regions. Calculations of the fluxes with ECMWF winds and vertical velocities shows that the eddy fluxes cannot be ignored in the variations of UTH, especially in the subtropical regions. However, the traditional analyses provide little information on the dynamics of UTH variations. Using the new algorithm of Zhu and Newell (1998), we find that the increase of moisture in the upper troposphere was contributed mostly by local convection over the scattered small areas less than 10 percent of the whole area, while the contribution of background fluxes and horizontal transport were relatively small.

Without using long term climatological data, this study may not suggest an essential difference between the feedbacks from the anomalous heating in a long-term climatology and in the seasonal cycles, since the long-term mean circulations and the interhemispheric transport do not play the most important role in the changes of UTH over the extratropical regions. It is possible that there is a limit of the positive feedback, over which an increase of SST will reduce UTH. However,

the limitation may be caused by multi physical processes much more complicated than the large scale subsidence.

The positive feedback of UTH from SST variations found here from the seasonal cycle does not nullify the existence of the negative feedback process suggested by Lindzen (1990). The increased tropical convection in the El Niño period enhanced the large scale subsidence in the subtropical latitudes. The total feedback depends on the comparison between the positive and negative feedbacks. Due to the local convection, the mean subsidence in the subtropical regions may not mean an over all downward transport of water vapor, even if the detrainment of clouds and evaporation in the free atmosphere are not considered. Although a positive feedback was suggested in the present study, the behaviors between the two hemispheres were different. Thus, a question may still remain: Does a possible manner of anomalous heating exist, which will lead to an over all negative feedback? The model experiments of Del Genio *et al.* (1996) found that the feedback of the greenhouse effect depends largely on the change of SST gradient.

When the feedback from the local SST is positive, the correlation to the remote deep convection may be negative. This prevents drawing a final conclusion on the greenhouse effect in terms of the feedback from remote deep convection. The heating caused by greenhouse gases may not be concentrated at a particular place. A low resolution model with simple physics may simulate the negative feedback but not the positive feedback. As convection over small areas has a great influence on the upper tropospheric water vapor distribution, the climate model needs to be of high resolution.

Although the lower boundary is covered mostly by ocean water in

the tropics, the circulations are highly asymmetric in the zonal direction, due to the local convection. The time and zonal mean shows that the whole atmosphere in the tropical and extratropical regions rises and sinks, respectively. Although this picture fits the time averaged energy balance equation, the mean Hadley cell may be far from the real climatology at a local place, and add little to our understanding for tropical dynamics. Using the mean circulation to replace the real circulation for the study of a nonlinear dynamic process may be misleading. For example, the time and zonal mean vertical velocities on 464 hPa evaluated by ECMWF data (Figure is not shown) were downward over most latitudes from 20°-40° in the same two seasons as in Figure 5, simultaneously, the mean water vapor transport was generally upward.

In the physical world, the large scale circulations in the extratropical atmosphere are characterized by slantwise circulations, as illustrated by Green *et al.* (1966) and shown by ECMWF data. When the subsidence heating is offset by radiative cooling, the cooling may take place also in the environment at a similar rate. Thus, the temporal air motions have the trajectories with slopes close to or less than those of isentropic surfaces in the statically stable atmosphere. This feature remains in the time-averaged circulations. The transport in the slantwise convection has both vertical and horizontal components, and the water vapor fluxes cannot be discussed with one-dimensional models.

The drying of the subtropical atmosphere may be carried out most efficiently by the stratospheric intrusion across the humidity surfaces at middle latitudes. This process is related to baroclinic perturbations and heat balance. The relation between increases of tropical deep

convection and baroclinic activity needs more study. As the tropics get extra heating, the meridional temperature gradient and northward heat transport increase. This result may facilitate the frontogenesis and baroclinic disturbance developments in the extratropical regions. The forming of dry anomalies in the El Niño episode suggest an increase of the baroclinic activity at middle latitudes. The intensified slantwise subsidence may cool rather than heat the local atmosphere.

Acknowledgements

Support for this work came from the NASA's Earth Science Enterprise through grant No. NAG 5-6710.

References

Allam,R.J. and A.F.Tuck (1984): Transport of water vapour in a stratosphere-troposphere general circulation model. I: Fluxes, *Quart. J. R. Met. Soc.*, **110**, 321-356.

Cess, R.D., G.L.Potter, J.P.Blanchet, G.J.Boer, A.D.Del Genio, M.Déqué, V.Dymnikov, V.Galin, W.L.Gates, S.J.Ghan, J.T.Kiehl, A.A.Lacis, H.Le Treut, Z-X.Li, X-Z.Liang, B.J.McAvaney, V.P.Meleshko, J.F.B.Mitchell, J-J.Morcrette, D.A.Randall, L.Rikus, E.Roeckner, J.F.Royer, U.Schlese, D.A.Sheinin, A.Slingo, A.P.Sokolov, K.E.Taylor, W.M.Washington, R.T.Wetherald, I.Yagai and M-H. Zhang (1990): Intercomparison and Interpretation of climate feedback processes in 19 atmospheric general circulation models, *J. Geophys. Res.*, **95**, 16601-16615.

Chiou,E.W., M.P.McCormick and W.P.Chu (1997): Global water vapor distributions in the stratosphere and upper troposphere derived from 5.5 years of SAGE II observations, *J. Geophys. Res.*, **102**, 19105-19118.

Chou,M-D. (1994): Coolness in the tropical Pacific during an El Niño episode, *J. Climate*, **7**, 1684-1692.

Del Genio, A.D, W.Kovari Jr. and M-S Yao (1994): Climatic implications of the seasonal variation of upper troposphere water vapor, *Geophys. Res. Lett.*, **21**, 2701-2704.

Del Genio, A.D, M-S Yao, W.Kovari Jr. and K.K-W.Lo (1996): A prognostic cloud water parameterization for global climate models, *J. Climate*, **9**, 270-304.

Eady,E.T.(1950): The cause of the general circulation of the atmosphere, *Centenary Proceedings*, Royal Meteorological Society, 156-172.

Fu,R, R.E.Dickinson and B. Newkirk (1997): Response of the upper tropospheric humidity and moisture transport to change of tropical convection. A comparison between observations and a GCM over an ENSO cycle. *Geophys. Res. Lett.*, **24**, 2371-2374.

Green,J.S.A., F.H.Ludlam and J.F.R.McIlveen (1966): Isentropic relative-flow analysis and the parcel theory, *Quart. J. Roy. Meteor. Soc.*, **92**, 210-219.

Lindzen,R.S. (1990): Some coolness concerning global warming, *Bull. Amer. Meteor. Soc.*, **71**, 288-299.

Newell,R.E., Y.Zhu, W.G.Read and J.W.Waters (1997): Relationship between tropical upper tropospheric moisture and eastern tropical Pacific sea surface temperature at seasonal and interannual time scales, *Geophys. Res. Lett.*, **24**, 25-28.

Newell,R.E., Y.Zhu, E.V.Browell, W.G.Read and J.W.Waters (1996): The Walker circulation and tropical upper tropospheric water vapor, *J. Geophy. Res.*, **101**, 1961-1974.

Palmén,E. and C.W.Newton (1969): *Atmospheric Circulation Sys-*

tems. Academic Press, 603pp.

Peixoto,J.P. and A.H.Oort (1992): *Physics of Climate*, American Institute of Physics, New York, 520pp.

Rasmusson,E.M. (1972): Seasonal variations of tropical humidity parameters, Chapter 5 in *The General Circulation of the Tropical Atmosphere*, (Volume 1, Newell,R.E., J.W.Kidson, D.G.Vincent and G.J.Boer Ed.). MIT Press, 258pp.

Raval,A. and V.Ramanathan (1989): Observational determination of the greenhouse effect, *Nature*, **342**, 758-761.

Read, W.G., J.W.Waters, D.A.Flower, L.Froidevaux, R.F.Jarnot, D.L.Hartmann, R.S.Harwood and R.B.Rood (1995): Upper troposphere water vapor from UARS MLS, *Bull. Amer. Meteor. Sco.*, **76**, 2381-2389.

Read, W.G. *et al.*, 1999: In preparation.

Riehl,H. and J.S.Malkus (1958): On the heat balance in the equatorial trough zone. *Geophysica*, **6**, 503-537.

Rind.D, E.W.Chiou, W.Chu, J.Larsen, S.Oltmans, J.Lerner, M.P.McCormick and L.McMaster (1990): Positive water vapour feedback in climate models confirmed by satellite data, *Nature*, **349**, 500-503.

Sandor,B.J., W.G.Read, J.W.Waters and K.H.Rosenlof (1998): Seasonal behavior of tropical to mid-latitude upper tropospheric water vapor from UARS MLS, submitted to *J. Geophys. Res.*.

Soden,B,J and R.Fu (1995): A satellite analysis of deep convection, upper-tropospheric humidity, and the greenhouse effect, *J. Climate*, **8**, 2333-2351.

Sun, D-Z. and R.S.Lindzen (1993): Distribution of tropical tropospheric water vapor, *J. Atmos. Sci.*, **50**, 1643-1660.

Zhu, Y. and R.E.Newell (1994): Atmospheric rivers and bombs, *Geophys. Res. Lett.*, **21**, 1999-2002.

Zhu, Y. and R.E.Newell (1998): A proposed algorithm for moisture fluxes from Atmospheric rivers, *Mon. Weath. Rev.*, **126**, 725-735.

Table Captions

Table 1, Convective and background upward MLS water vapor fluxes, across 464 hPa for 1991-1992 in a) and for 1992-1993 in b); c) is the vertical fluxes across 316 hPa for 1991-1992. The numbers in parenthesis are the convective fluxes within 20°S-20°N.

Table 2, Meridional and vertical influxes of MLS water vapor into the layer, from 464 hPa to 150 hPa for 1991-1992 in a) and 1992-1993 in b); c) is from 316 hPa to 150 hPa for 1991-1992. The numbers in parenthesis are the net influxes. The annual mean influxes are converted into equivalent precipitation down from 464 hPa in a) and b), but from 316 hPa in c).

Figure Captions

Figure 1: The differences of one-season climatologies. Red contours depict the seasonal mean SST in 12/91-02/92 minus that in 12/93-02/94, units: C°. The difference of MLS water vapor column content within 316-147 hPa is in green, units: 0.1kg/m^2.

Figure 2: MLS UTH fluxes by ECMWF winds, blue: time and zonal mean flow fluxes, red: transient perturbation fluxes, green: stationary eddy fluxes, and black heavy: the total mean fluxes. a) Northward fluxes integrated from 464 hPa to 147 hPa for 1991-1992, b) the same as a) but for 1992-1993, c) upward fluxes on 464 hPa for 1991-1992, and d) the same as c) but for 1992-1993.

Figure 3: MLS water vapor column content in 316-417 hPa, solid: 1991-1992 and dashed: 1993-1994.

Figure 4: Upward fluxes of water vapor on 500 hPa over a tropospheric river in units 10^{-6} kg/(m^2s), evaluated from ECMWF data at 12Z on January 4, 1992. The vectors represent the horizontal vapor fluxes integrated from 1000 to 300 hPa in units where the maximum vector is 1160 kg/(m.s).

Figure 5: Partitioned upward MLS UTH fluxes on 464 hPa, solid thin: convective flux, dashed: background flux. The total fluxes represented the heavy curves are the same as in Figure 2b.

Figure 6: The subtropical slantwise convection in the monthly mean ECMWF fields during January, 1992. a) Mean MLS UTH (green, ppmv), potential temperature (red, K), potential vorticity (blue, 10^{-7} Km^2/(kg.s)) and air velocity vectors (Maximum vector is 10 m/s). The interval of UTH contours is 500 ppmv over the level of 500 ppmv. The black circles indicate the subtropical westerly jets, of which the speeds

(m/s) are shown at the centers. b) Streamlines on 150 hPa. Maximum vector is 75 m/s. c) Cross-section of potential temperature (K) and air velocity (m/s) along the green line in b). Maximum vector is 63 m/s.

Figure 7: Time series of ECMWF vertical velocity, specific humidity and relative humidity on 300 hPa in June, 1992.

Table 1*a*: Convective and background upward MLS water vapor fluxes across 464 hPa for 1991-1992. The numbers in parenthesis are the convective fluxes within 20°S-20°N.

Convective F_z *Background* F_z 10^6 kg/s	40S-20S	20S-Eq	Eq-20N	20N-40N
12/91-02/92	123 **-44**	**(484)** 358 *27*	126 *13*	65 **-19**
03/92-05/92	103 **-21**	**(435)** 237 *16*	198 *12*	87 **-35**
06/92-08/92	45 *6*	(338) 42 **-21**	**296** *103*	112 *4*
09/92-11/92	80 *7*	(341) 105 **-26**	**236** *93*	78 **-17**
Annual mean	88 *-14*	(399) 185 *-1*	214 *55*	85 *-17*

Table 1*b*: Convective and background upward MLS water vapor fluxes across 464 hPa for 1992-1993. The numbers in parenthesis are the convective fluxes within 20°S-20°N.

Convective F_z *Background* F_z 10^6 kg/s	40S-20S	20S-Eq	Eq-20N	20N-40N
12/92-02/93	**93** *4*	(373) **270** *49*	103 *30*	54 *-6*
03/93-05/93	74 *3*	(326) 181 *26*	145 *53*	59 *-10*
06/93-08/93	54 *1*	(358) 62 **-24**	**296** *97*	**110** *6*
09/93-11/93	72 *9*	(408) 104 **-56**	**304** *71*	75 **-72**
Annual mean	73 *4*	(380) 154 *-1*	212 *62*	74 *-21*

Table 1c: Convective and background upward MLS water vapor fluxes across 316 hPa for 1991-1992. The numbers in parenthesis are the convective fluxes within 20°S-20°N.

Convective F_z *Background* F_z 10^6 kg/s	40S-20S	20S-Eq	Eq-20N	20N-40N
12/91-02/92	17 **-13**	(**78**) 59 *0*	19 *-4*	6 **-5**
03/92-05/92	14 **-9**	(**70**) 37 *0*	33 *-1*	12 **-7**
06/92-08/92	7 *-1*	(58) 5 **-8**	**53** *10*	21 **-4**
09/92-11/92	11 *-1*	(57) 16 **-8**	**41** *9*	9 **-7**
Annual mean	12 *-6*	(65) 29 *-4*	37 *3*	12 *-6*

Table 2*a*: Meridional and vertical influxes of MLS water vapor into the layer from 464 hPa to 150 hPa for 1991-1992. The numbers in parenthesis are the net influxes.

Influx of F_y *Influx of* F_z 10^6 kg/s	40S-20S	20S-Eq	Eq-20N	20N-40N
12/91-02/92	-17	-43	-22	21
	78	**385**	*139*	*46*
Net influxes	(61)	(**342**)	(117)	(67)
03/92-05/92	-4	-41	-32	6
	82	*254*	*209*	*52*
Net influxes	(78)	(213)	(177)	(58)
06/92-08/92	9	5	-46	0
	49	*20*	**399**	**115**
Net influxes	(58)	(25)	(**353**)	(**115**)
09/92-11/92	-9	-4	-53	-2
	88	*79*	*330*	*61*
Net influxes	(**79**)	(75)	(276)	(59)
Annual mean	5	-21	-38	6
	74	*185*	*270*	*68*
Net influxes	(69)	(164)	(232)	(74)
P_e (mm/year)	(28)	(59)	(83)	(31)

Table 2*b* Meridional and vertical influxes of MLS water vapor into the layer from 464 hPa to 150 hPa for 1992-1993. The numbers in parenthesis are the net influxes.

Influx of F_y *Influx of* F_z 10^6 kg/s	40S-20S	20S-Eq	Eq-20N	20N-40N
12/92-02/93	-15	-31	-41	27
	97	**319**	*133*	*48*
Net influxes	(**82**)	(**287**)	(92)	(75)
03/93-05/93	-9	-40	-30	16
	77	*207*	*198*	*49*
Net influxes	(68)	(167)	(167)	(64)
06/93-08/93	5	4	-45	-5
	56	*38*	**394**	**116**
Net influxes	(61)	(43)	(**348**)	(**112**)
09/93-11/93	-22	-5	-54	-19
	81	*48*	*375*	*3*
Net influxes	(59)	(43)	(321)	(-16)
Annual mean	-10	-18	-43	5
	78	*153*	*275*	*54*
Net influxes	(67)	(135)	(232)	(59)
P_e (mm/year)	(28)	(49)	(84)	(24)

Table 2c: Meridional and vertical influxes of MLS water vapor into the layer, from 316 hPa to 150 hPa for 1991-1992. The numbers in parenthesis are the net influxes.

Influx of F_y *Influx of* F_z 10^6 kg/s	40S-20S	20S-Eq	Eq-20N	20N-40N
12/91-02/92	3	-20	4	8
	4	**59**	*15*	*1*
Net influxes	(7)	(**39**)	(19)	(9)
03/92-05/92	4	-12	-7	5
	5	*37*	*32*	*5*
Net influxes	(10)	(25)	(25)	(10)
06/92-08/92	4	12	-18	1
	6	*-3*	**63**	*17*
Net influxes	(10)	(9)	(**45**)	(*17*)
09/92-11/92	0	5	-16	2
	10	*8*	*50*	*2*
Net influxes	(10)	(13)	(34)	(4)
Annual mean	3	-4	-9	4
	6	*25*	*40*	*6*
Net influxes	(9)	(21)	(31)	(10)
P_e (mm/year)	(4)	(8)	(11)	(4)

Figure 1, The differences of one-season climatologies

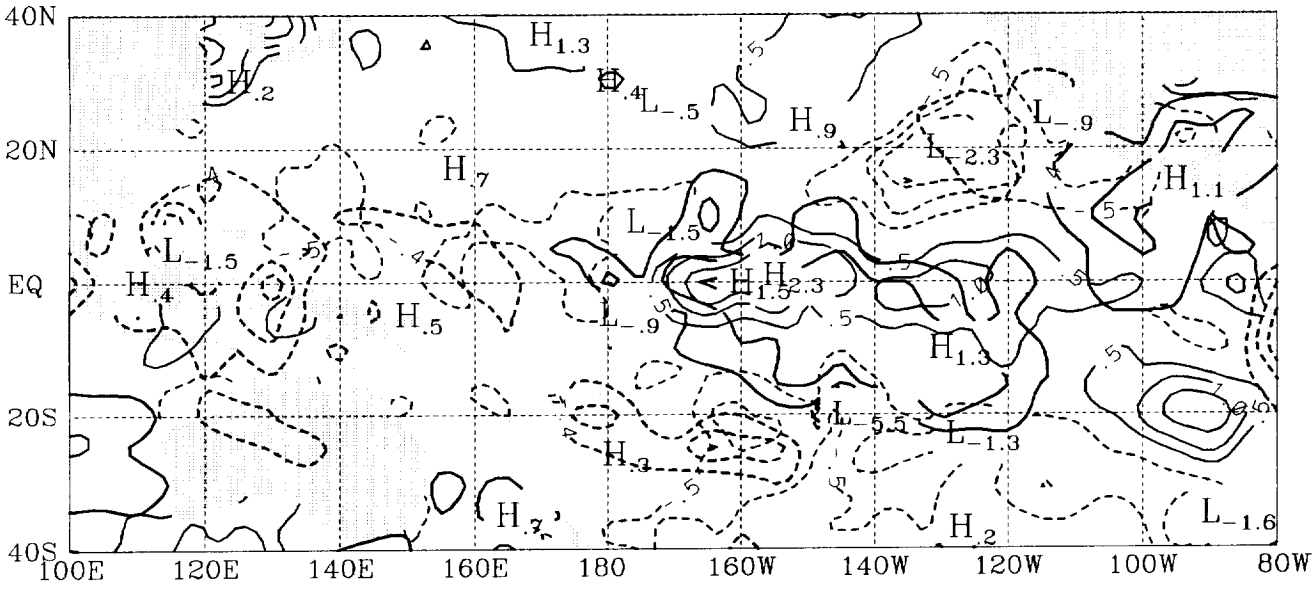

Figure 2a, Northward MLS UTH fluxes from 464 hPa to 147 hPa for 1991-1992

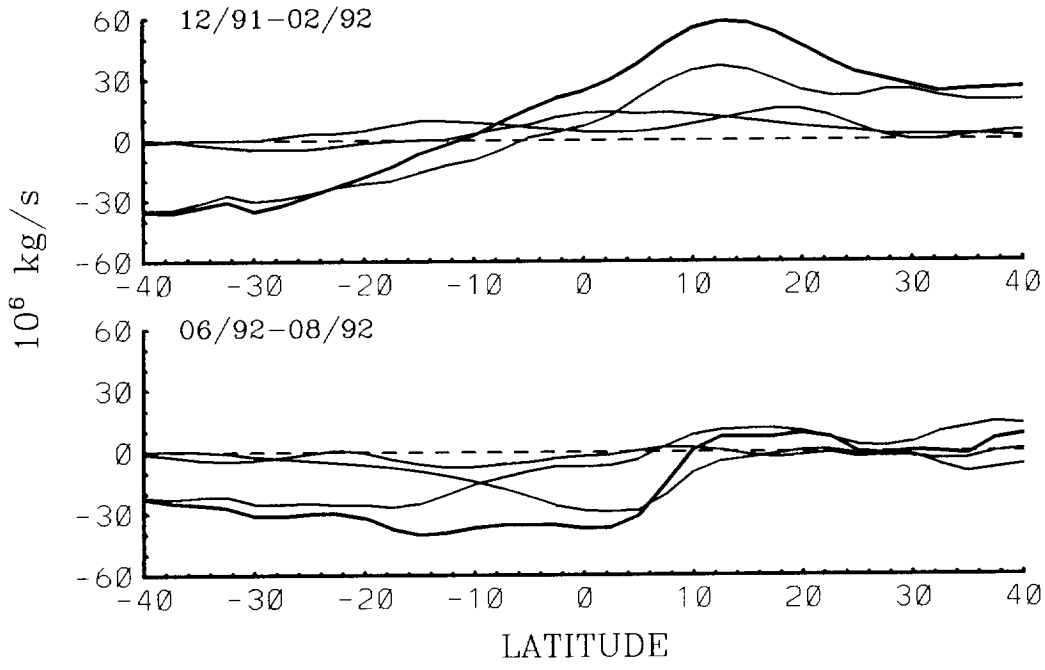

Figure 2b, Northward MLS UTH fluxes from 464 hPa to 147 hPa for 1992-1993

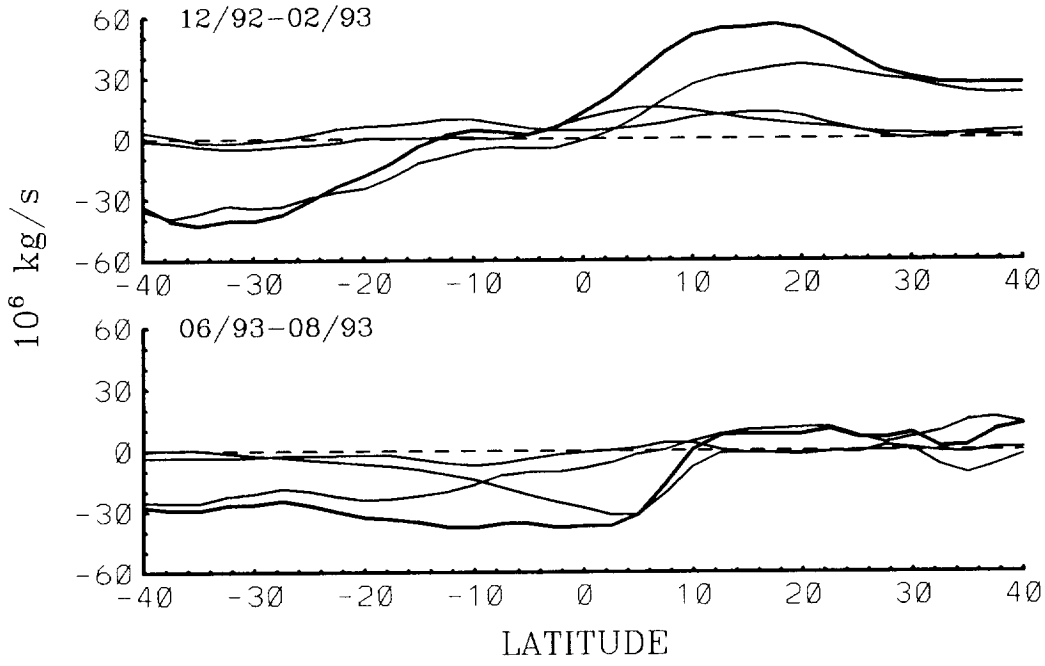

Figure 2c, Vertical MLS H_2O fluxes on 464 hPa for 1991-1992

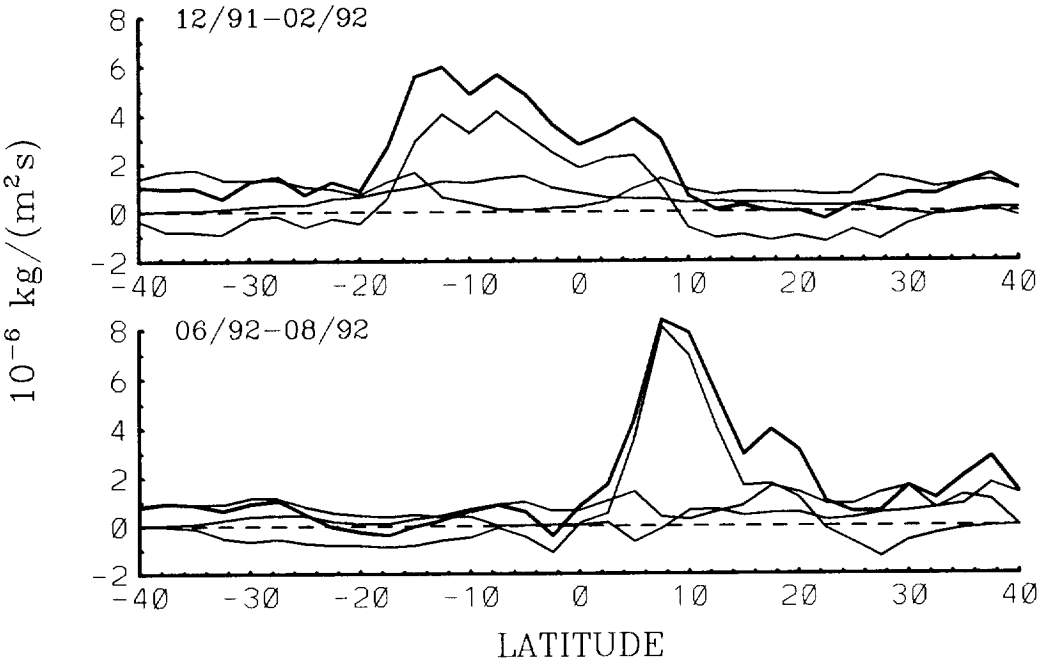

Figure 2d, Vertical MLS H_2O fluxes on 464 hPa for 1992–1993

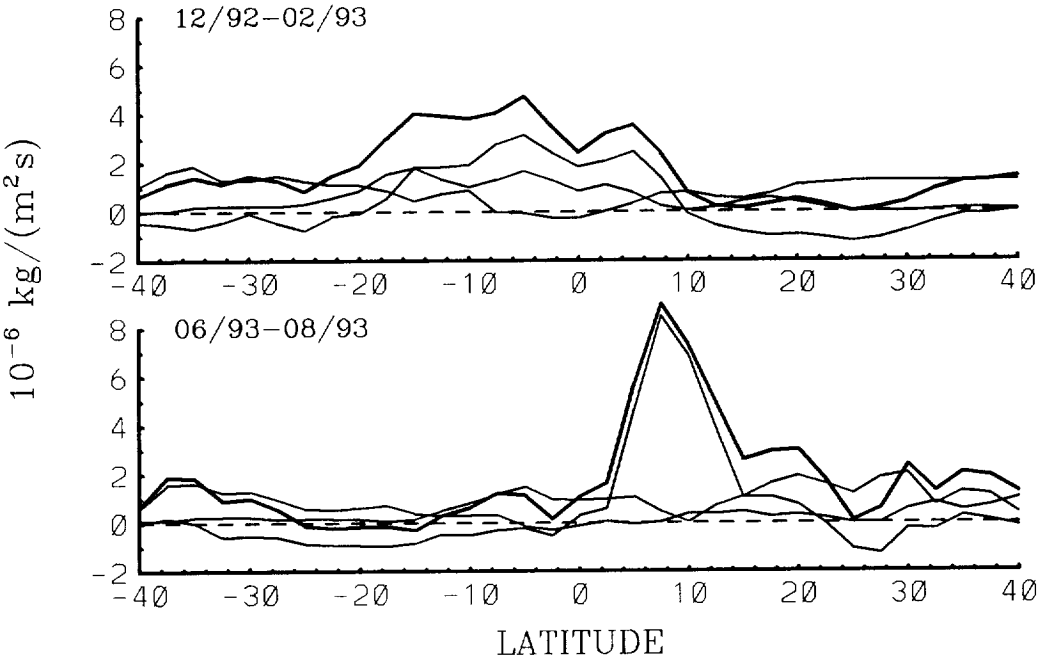

Figure 3, MLS H_2O column content in 316–147 hPa

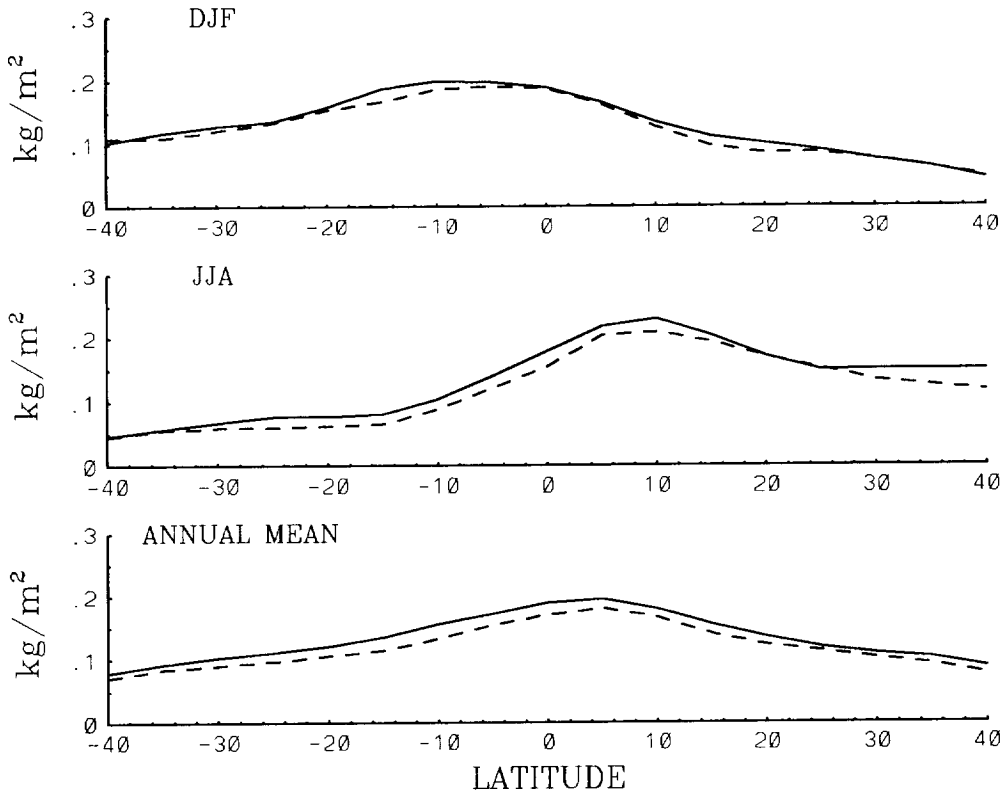

Figure 4, Upward fluxes of water vapor on 500 hPa over a tropospheric river
500 hPa, 1200UTC, 01/04/92

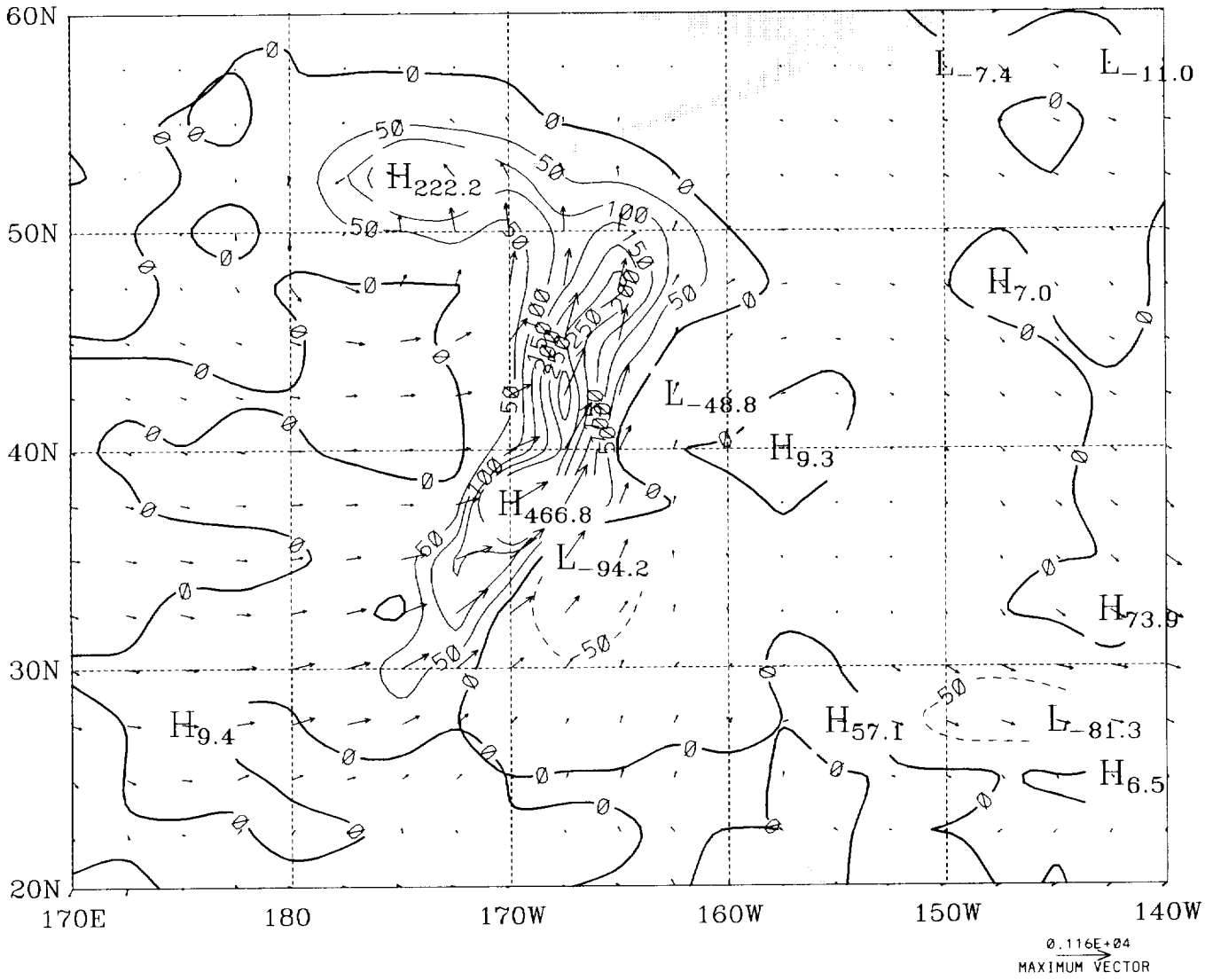

Figure 5, Partitioned upward MLS UTH fluxes on 464 hPa

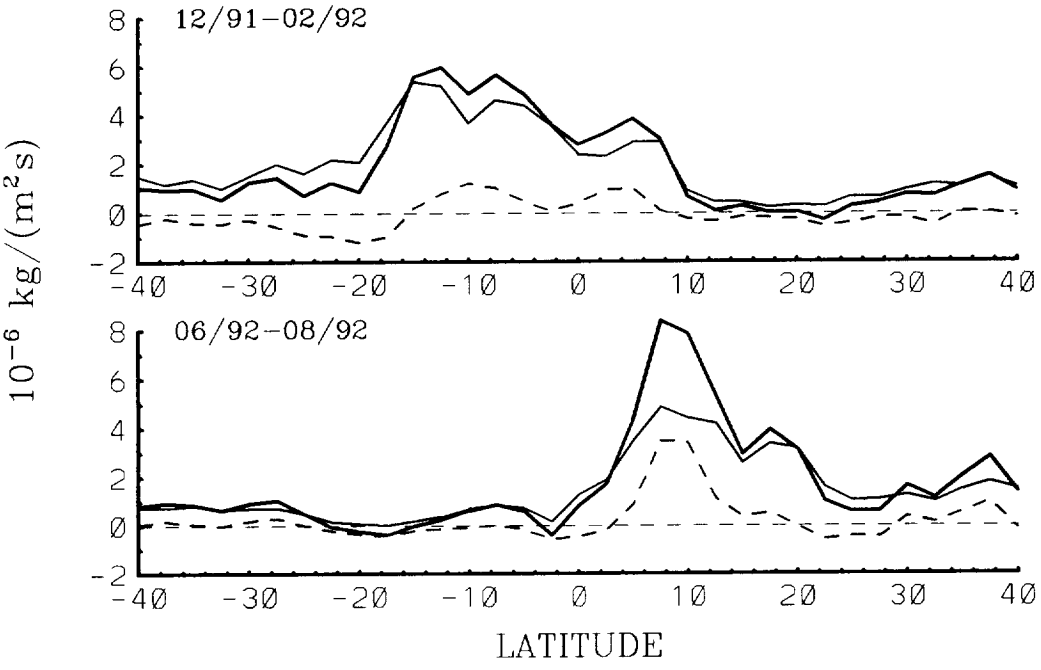

Figure 6a, The subtropical slantwise convection during January, 1992

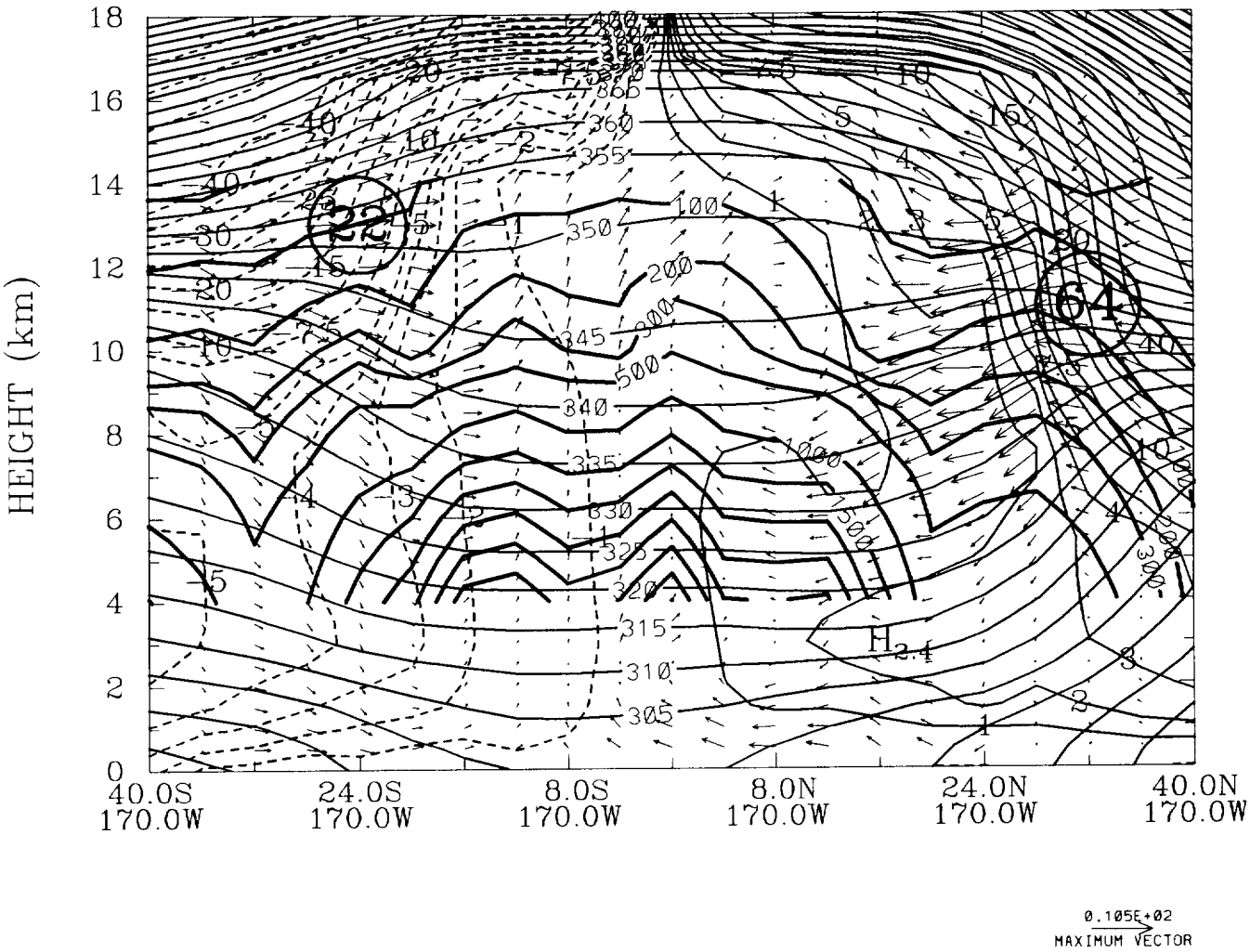

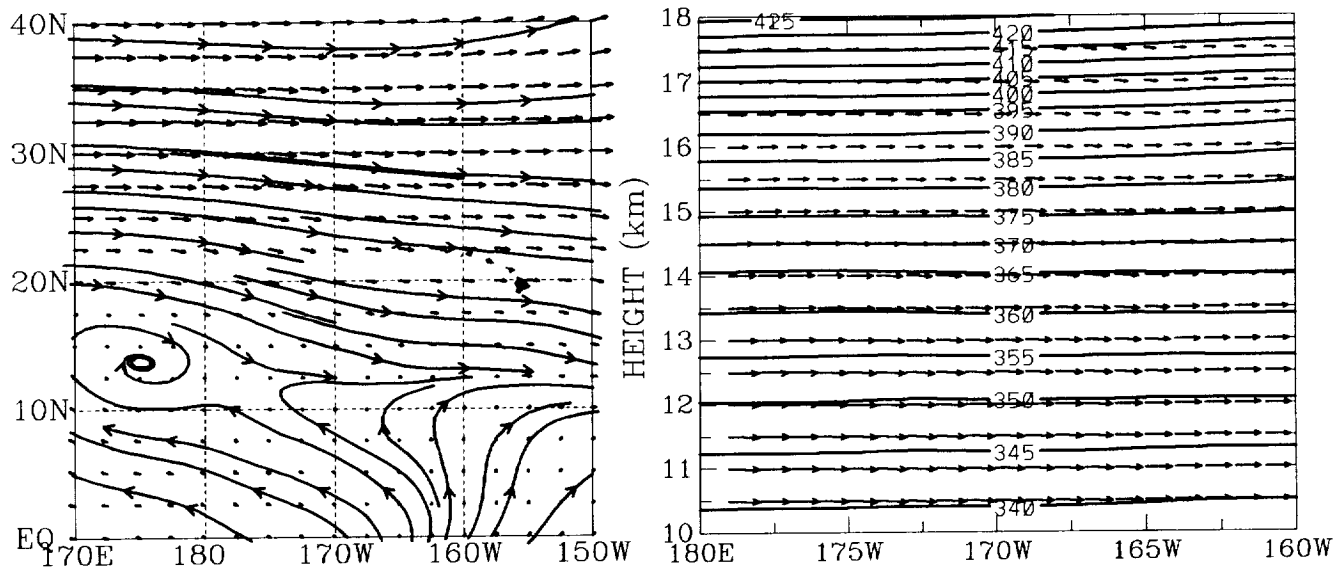
40N
30N
20N
10N
EQ
170E
180
170W
160W
150W
HEIGHT (km)
18
17
16
15
14
13
12
11
10
425
420
415
410
405
400
395
390
385
380
375
370
365
360
355
350
345
340
180E
175W
170W
165W
160W
0.628E+02
MAXIMUM VECTOR

Figure 7, Time series of ECMWF w, q and RH on 300 hPa in June, 1992